Figures and figure supplements

In silico screening by AlphaFold2 program revealed the potential binding partners of nuage-localizing proteins and piRNA-related proteins

Shinichi Kawaguchi and Xin Xu *et al*.

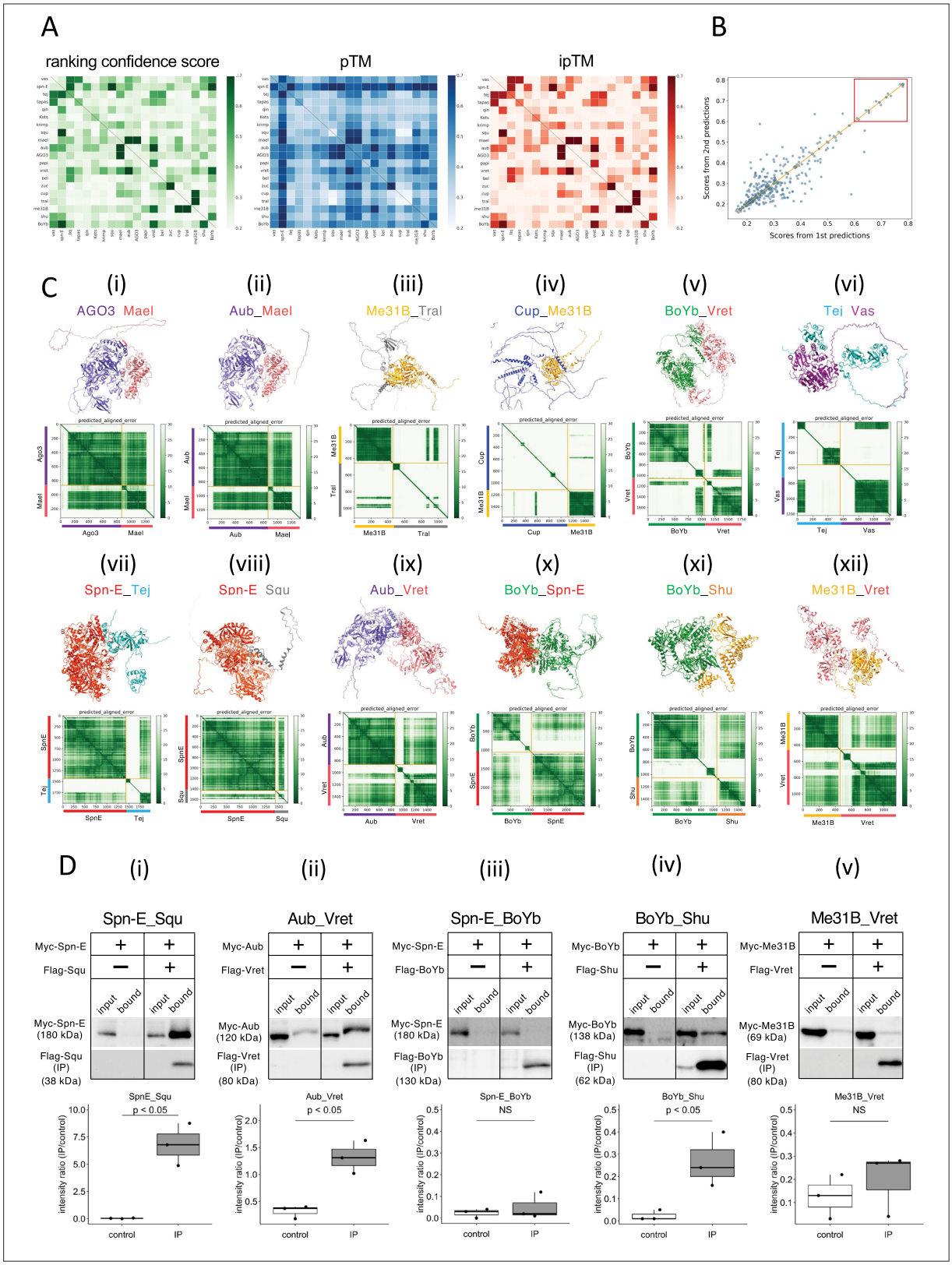

Figure 1. The 1:1 dimer structure prediction by AlphaFold2 for piRNA-related proteins. (**A**) Heatmaps of the prediction confidence scores (ranking confidence, green), pTM values (blue), and ipTM values (red) provided by AlphaFold2. The 20 types of proteins are aligned from top to bottom and left to right in the same order. Boxes on diagonal line represent homodimers. (**B**) Scatter plot of the ranking confidences. The scores from first and second predictions for each heterodimer pair are plotted on X and Y axis, respectively. (**Ci~xii**) The predicted 3D structures (top panels) and the Predicted

Figure 1 continued on next page

Figure 1 continued

Aligned Error (PAE) plots (bottom panels) for each candidate heterodimers scoring above 0.6. The PAE plot displays the positional errors between all amino acid residue pairs, formatted in a matrix layout. (**D**) Co-immunoprecipitation assays using tagged proteins to verify interactions between specific pairs: Spn-E_Squ (**i**), Aub_Vret (**ii**), Spn-E_BoYb (**iii**), BoYb_Shu (**iv**), and Me31B_Vret (**v**). Single transfected cells expressing only Myc-tagged but not Flag-tagged proteins are used as negative controls for each set. Box and whisker plots show the intensity ratio between immunoprecipitated and input bands (n = 3 biological replicates). p-values were calculated using Student's *t*-test.

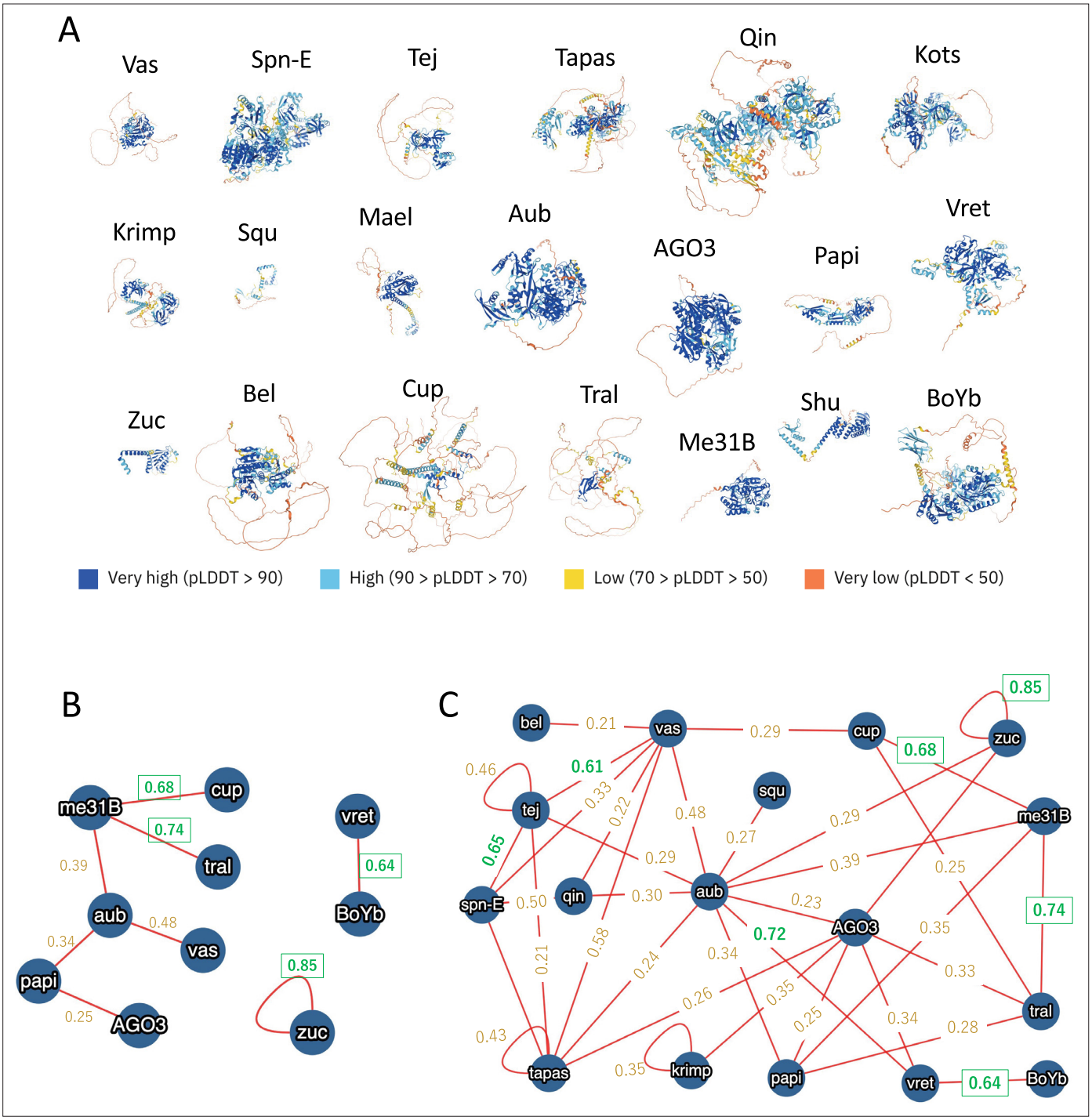

Figure 1—figure supplement 1. The nuage proteins analyzed in this study. (**A**) Predicted monomeric structures of 20 proteins used in this study, presented as ribbon models scaled uniformly. Residues are colored by per-residue model confidence scores (pLDDT). (**B**) Direct binding pairs from the MIST database, shown with AlphaFold2 scores. (**C**) Direct or indirect binding pairs from the MIST database, shown with AlphaFold2 scores.

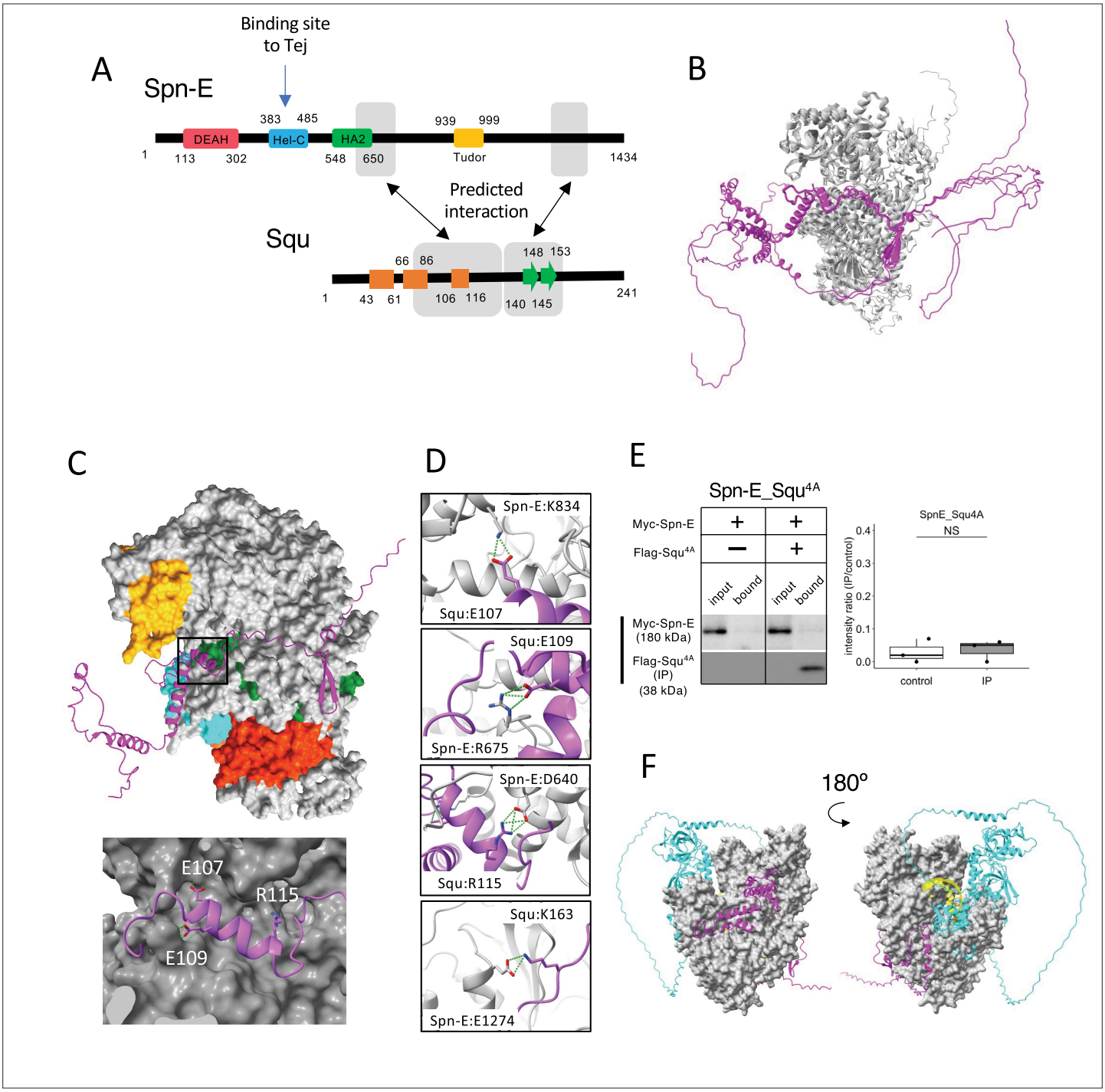

Figure 2. Interaction between Spn-E and Squ. (**A**) Schematic of Spn-E domain structures defined in SMART (***Letunic et al., 2021***). Boxes (α-helix: orange) and arrow (β-sheet: green) for Squ structure. The predicted interacting regions between Spn-E and Squ are indicated in gray boxes. Tej interaction site of Spn-E is also shown (***Lin et al., 2023***). (**B**) The predicted five models of heterodimer of Spn-E (in gray) and Squ (in magenta). Spn-E molecules in all five models are superimposed. (**C**) 3D structure of the Spn-E_Squ dimer colored by Spn-E domains as indicated in (**A**), with Squ in magenta. The enlarged image of the interface indicated by box is also shown. (**D**) The predicted salt bridges at the interface, with Spn-E in gray and Squ in magenta. The residues forming salt bridges are depicted in stick model. (**E**) Co-immunoprecipitation assay using S2 cell lysate to examine the interaction between Myc-Spn-E and Flag-Squ mutant (4A) whose salt bridge-forming residues are mutated to Ala. S2 cells expressing Myc-Spn-E alone is used as a control. The ratios of the band intensity (IP/input) are shown in a box and whisker plot (n = 3 biological replicates). p-values were calculated using Student's *t*-test. (**F**) The heterotetramer model of Spn-E_Squ_Tej_RNA predicted by AlphaFold3. Spn-E is shown as a space filled model in gray, Squ in magenta, Tej in cyan, and RNA in yellow. The model on the left is rotated 180° in the Y axis to produce the image on the right.

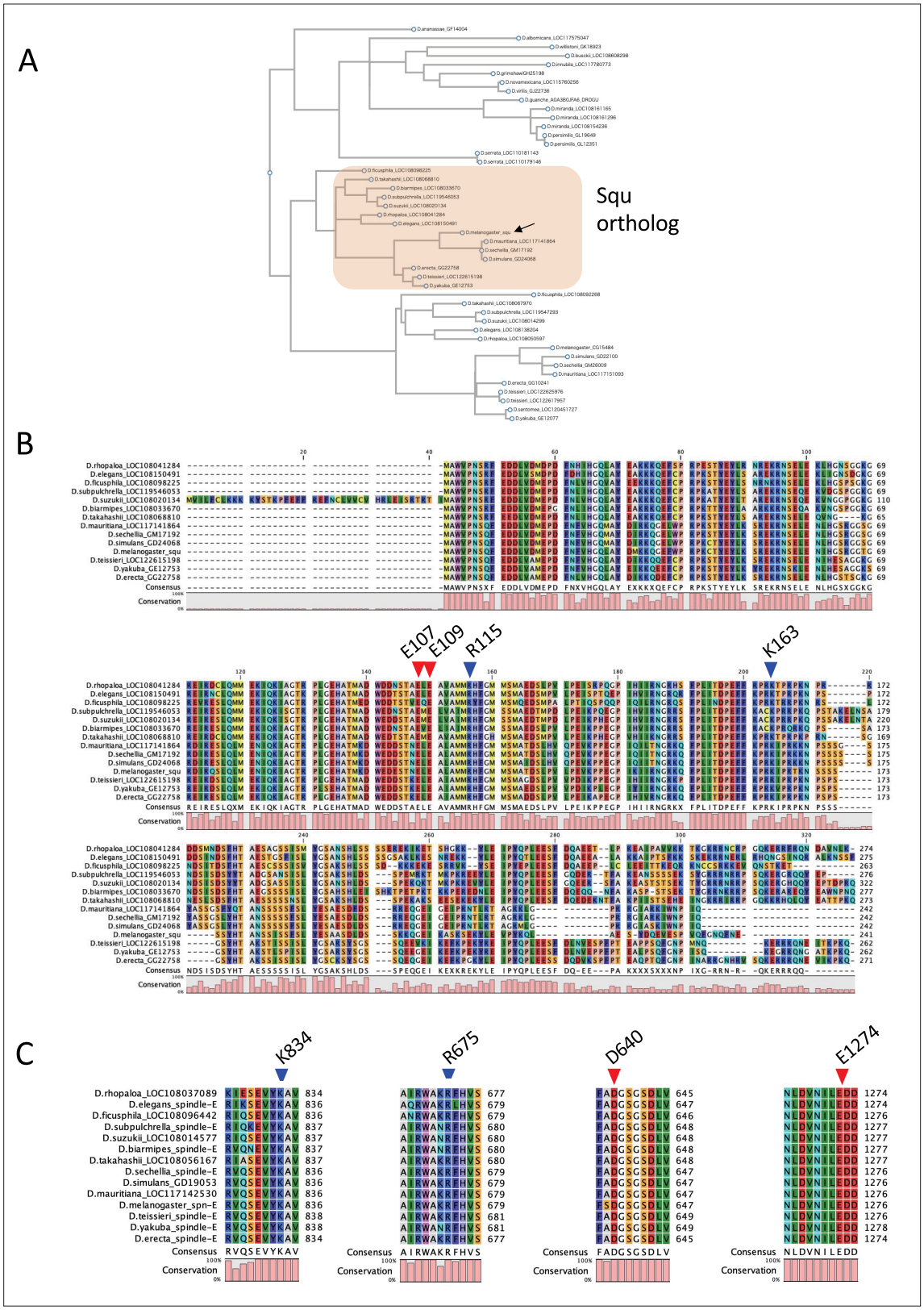

Figure 2—figure supplement 1. Comparative analysis of Squ and Spn-E orthologs in *Drosophila*. (**A**) Phylogenetic tree of Squ homologs across various Drosophila species. (**B**) Multiple sequence alignment of Squ orthologs from different *Drosophila* species, highlighting residues predicted to form salt bridges with Spn-E. (**C**) Multiple sequence alignment of Spn-E orthologs in *Drosophila* species focusing on regions around residues predicted to interact with Squ. The legend was shown in the original pdf, but the legends has been removed during the process.

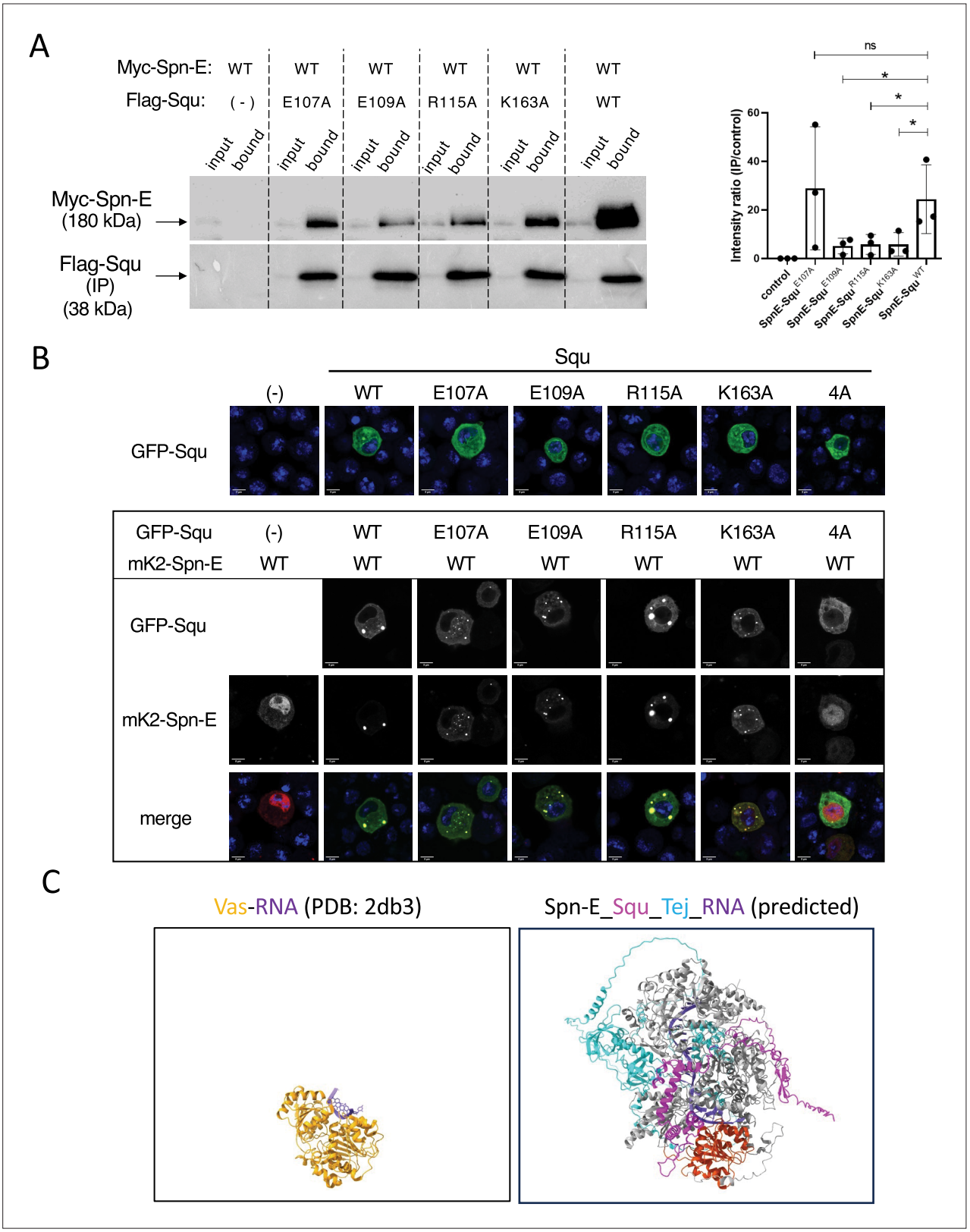

Figure 2—figure supplement 2. Interaction and localization analysis of Spn-E and Squ in S2 cells. (**A**) Co-immunoprecipitation of Myc-Spn-E and Flag-Squ expressed in S2 culture cells. In addition to the wildtype, Squ mutants containing amino acid residues predicted to form salt bridges altered to Alanine were also examined. The right panel shows quantifications of the intensity ratio (IP/input) with error bars indicating s.d. (n=3). ns: not significant. *: p-value < 0.10. (**B**) Localization of GFP-Squ wildtype and mutants in S2 cells (upper panels). Scale bars: 5 μm. Co-localization of mK2-Spn-E and GFP-

Figure 2—figure supplement 2 continued on next page

Figure 2—figure supplement 2 continued

Squ wildtype or mutant proteins (except for the 4A mutant) are shown in lower panels. Scale bars: 5 μm. (**C**) Structural comparison of the Vasa-ssRNA complex (PDB: 2db3, left) and the predicted SpnE_Squ_Tej_RNA complex by AlphaFold3 (right). The Spn-E helicase domain is highlighted in red, with Vas superimposed for comparison. Both views are from the same orientation.

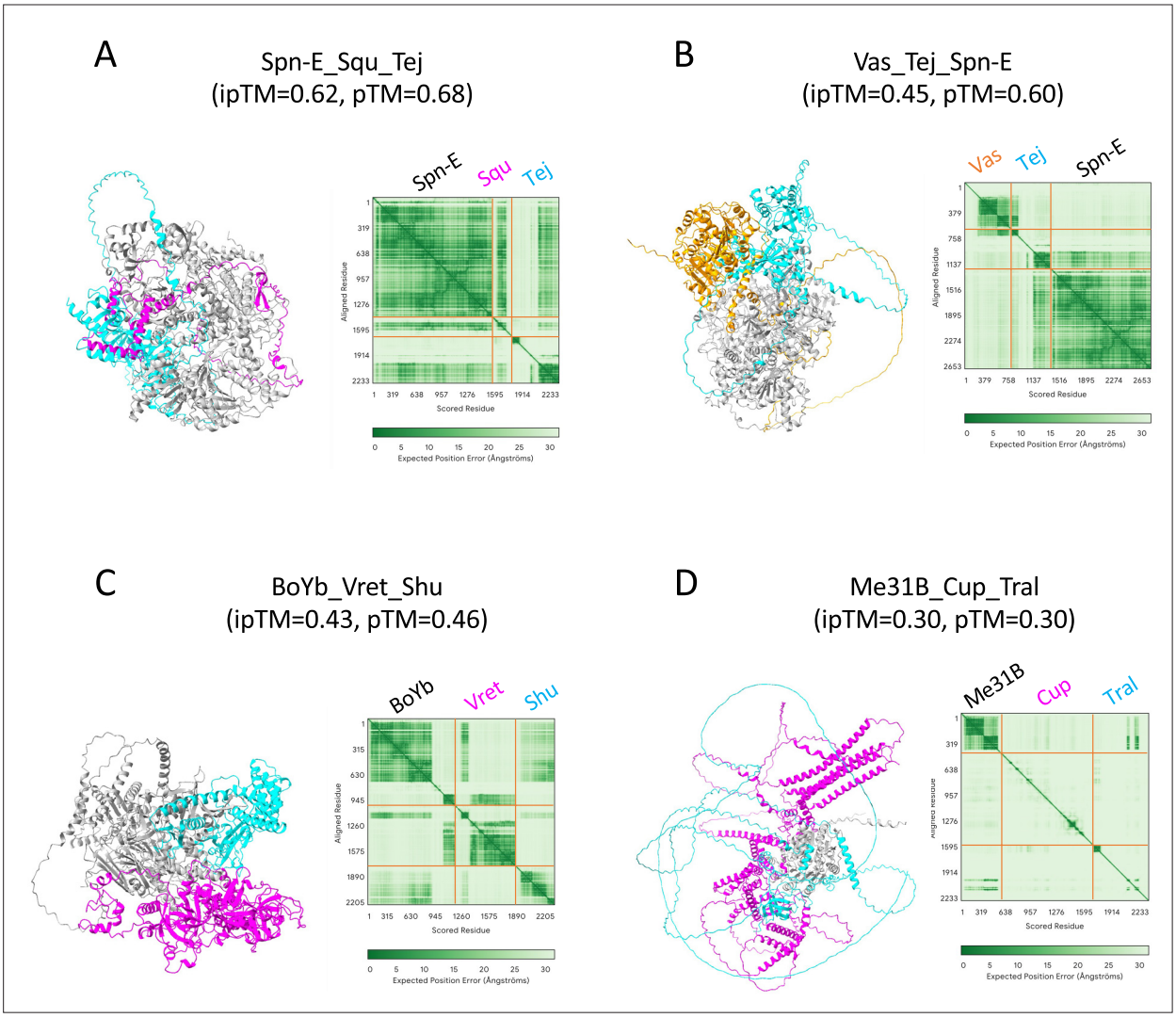

Figure 2—figure supplement 3. Trimer structures predicted by AlphaFold3. (**A**) SpnE_Squ_Tej. (**B**) Vas_Tej_Spn-E. (**C**) BoYb_Vret_Shu. (**D**) Me31B_Cup_Tral.PAE plots are also shown on the right. Orange lines indicate the protein boundaries.

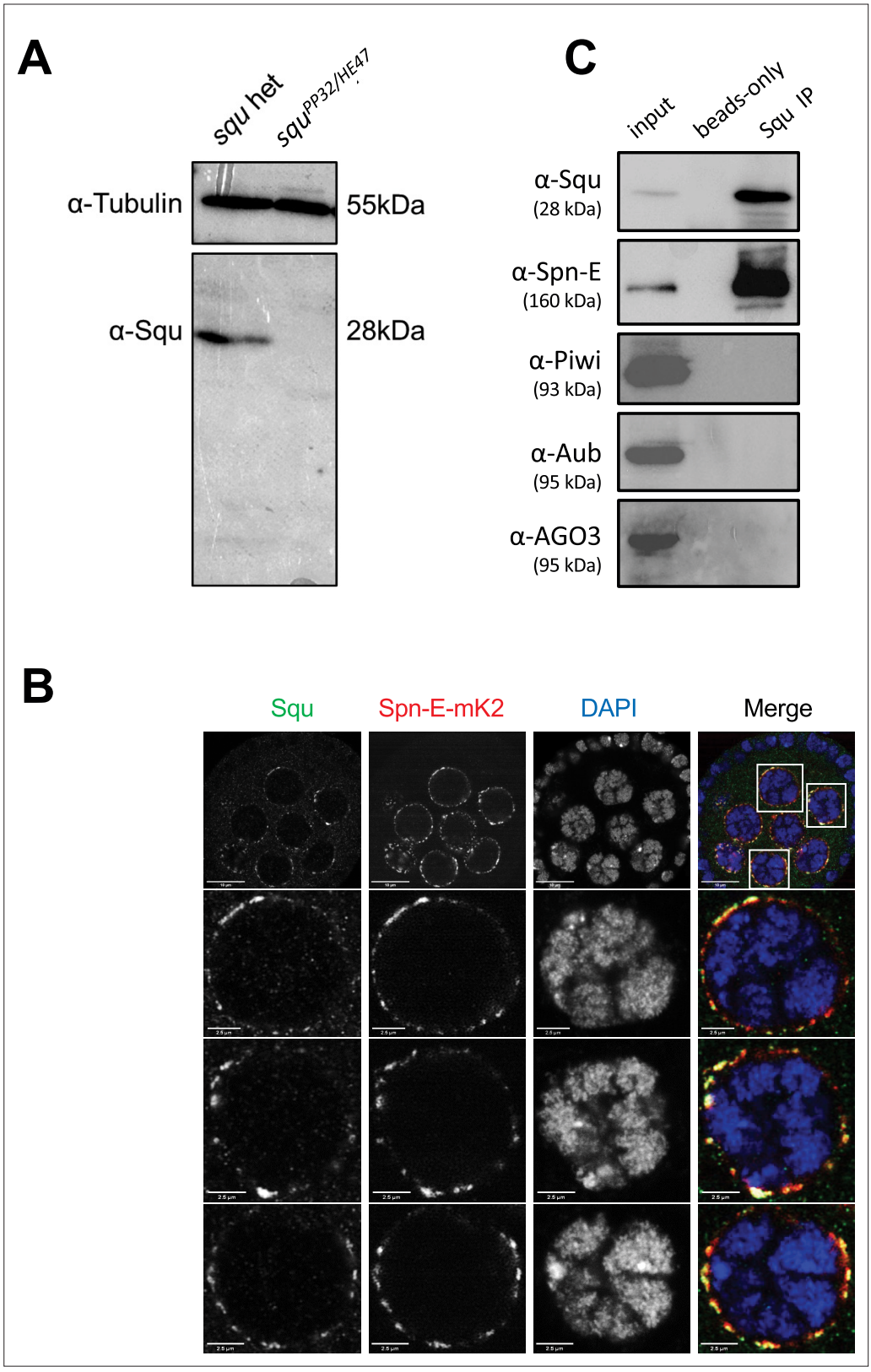

Figure 3. Spn-E and Squ interact in *Drosophila* ovary. (**A**) Western blotting analysis using anti-Squ antibody reveals a specific band at the expected size (approximately 28 kDa) for endogenous Squ in *Drosophila* ovarian lysates of the heterozygous control. This band is absent in the transheterozygote, *squ*$^{PP32/HE47}$. (**B**) Immunostaining of *Drosophila* egg chambers with anti-Squ antibody and anti-mKate2 (mK2) antibody demonstrates colocalization

Figure 3 continued on next page

Figure 3 continued

of Squ and Spn-E-mK2 in nuage, a perinuclear granule in germline cells. The enlarged images of nuclei are shown in the panels below. Scale bars: 10 μm (top row), 2.5 μm (enlarged images). (**C**) Immunoprecipitation of the endogenous Squ from ovarian lysate revealed the interaction with Spn-E protein. Proteins were detected by western blotting analysis using the specific antibody for each protein. The negative control was performed without anti-Squ antibody (beads only).

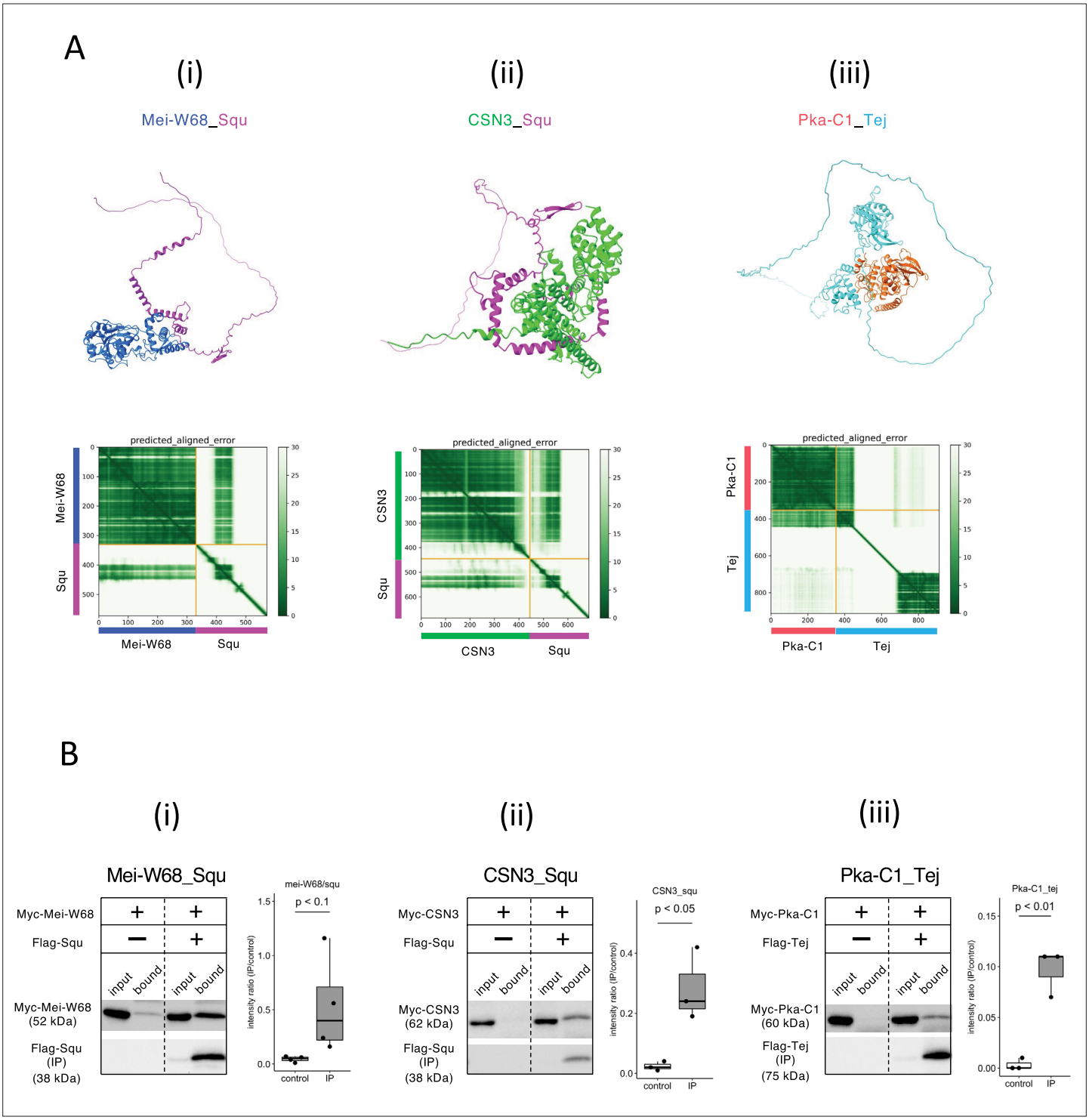

Figure 4. Squ- and Tej-interacting proteins predicted by AlphaFold2. (**Ai–iii**) The predicted dimer structures (top) and Predicted Aligned Error (PAE) plots (bottom) of Mei-W68 in blue and Squ in magenta (**i**), CSN3 in green and Squ in magenta (**ii**), Pka-C1 in orange and Tej in cyan (**iii**). The PAE plot displays the positional errors between all amino acid residue pairs, formatted in a matrix layout. (**Bi–iii**) Co-immunoprecipitation assays using tagged proteins to verify interactions between specific pairs: Mei-W68_Squ (**i**), CSN3_Squ (**ii**), and Pka-C1_Tej (**iii**). Single transfected cells expressing only Myc-tagged but not Flag-tagged proteins are used as negative controls for each set. Box and whisker plots show the intensity ratio between immunoprecipitated and input bands (n = 3 biological replicates). p-values were calculated using Student's *t*-test.

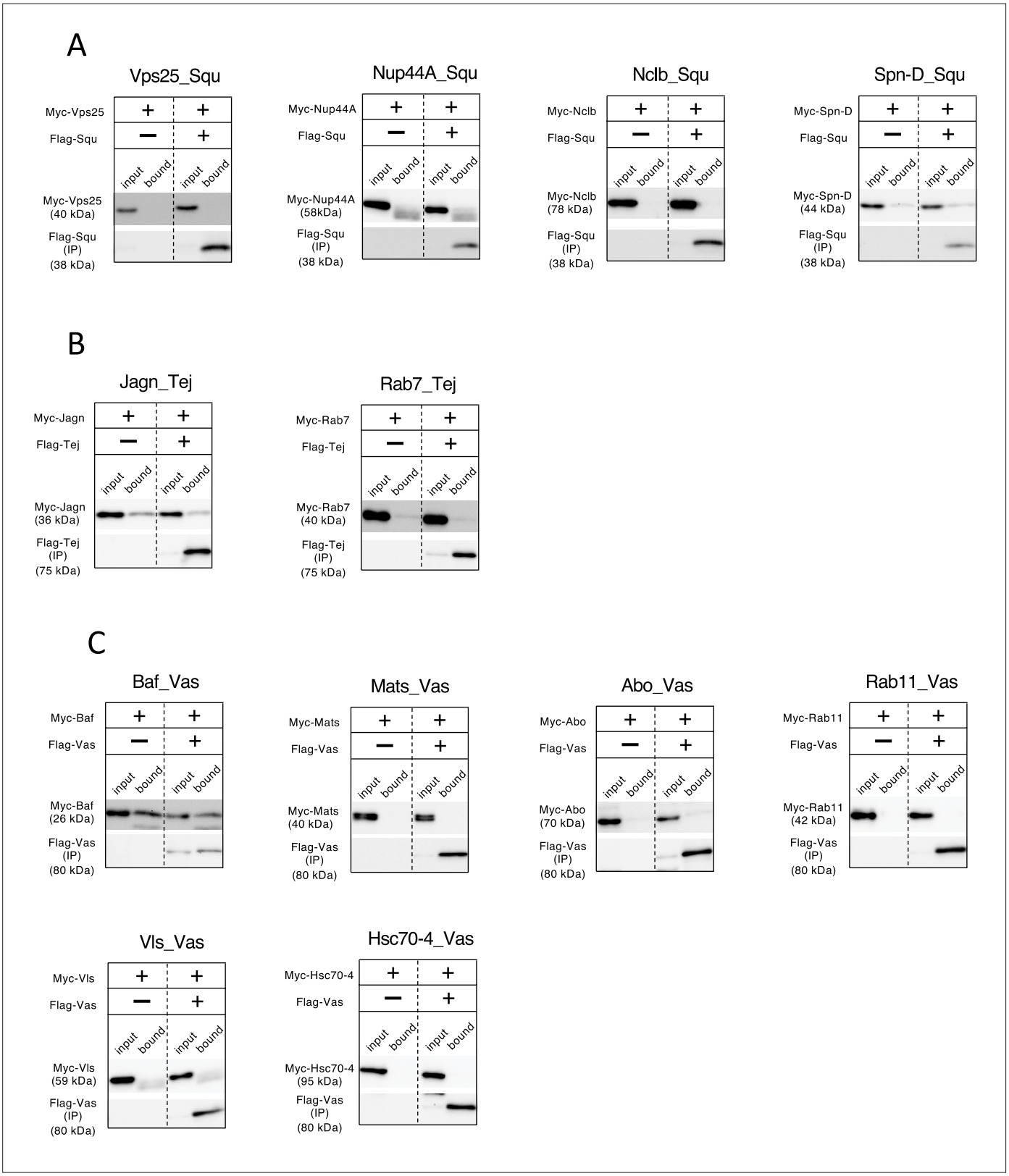

Figure 4—figure supplement 1. Validation of predicted protein interactions via co-immunoprecipitation from S2 cell lysate. (**A**) Examination of Squ-interacting candidates predicted by AlphaFold2. (**B**) Examination of Tej-interacting candidates predicted by AlphaFold2. (**C**) Examination of Vas-interacting candidates predicted by AlphaFold2.In all the experiments, Flag-tagged proteins are immunoprecipitated and blotted with anti-Myc and anti-Flag antibodies. Single-transfection of Myc-tagged proteins serve as controls.

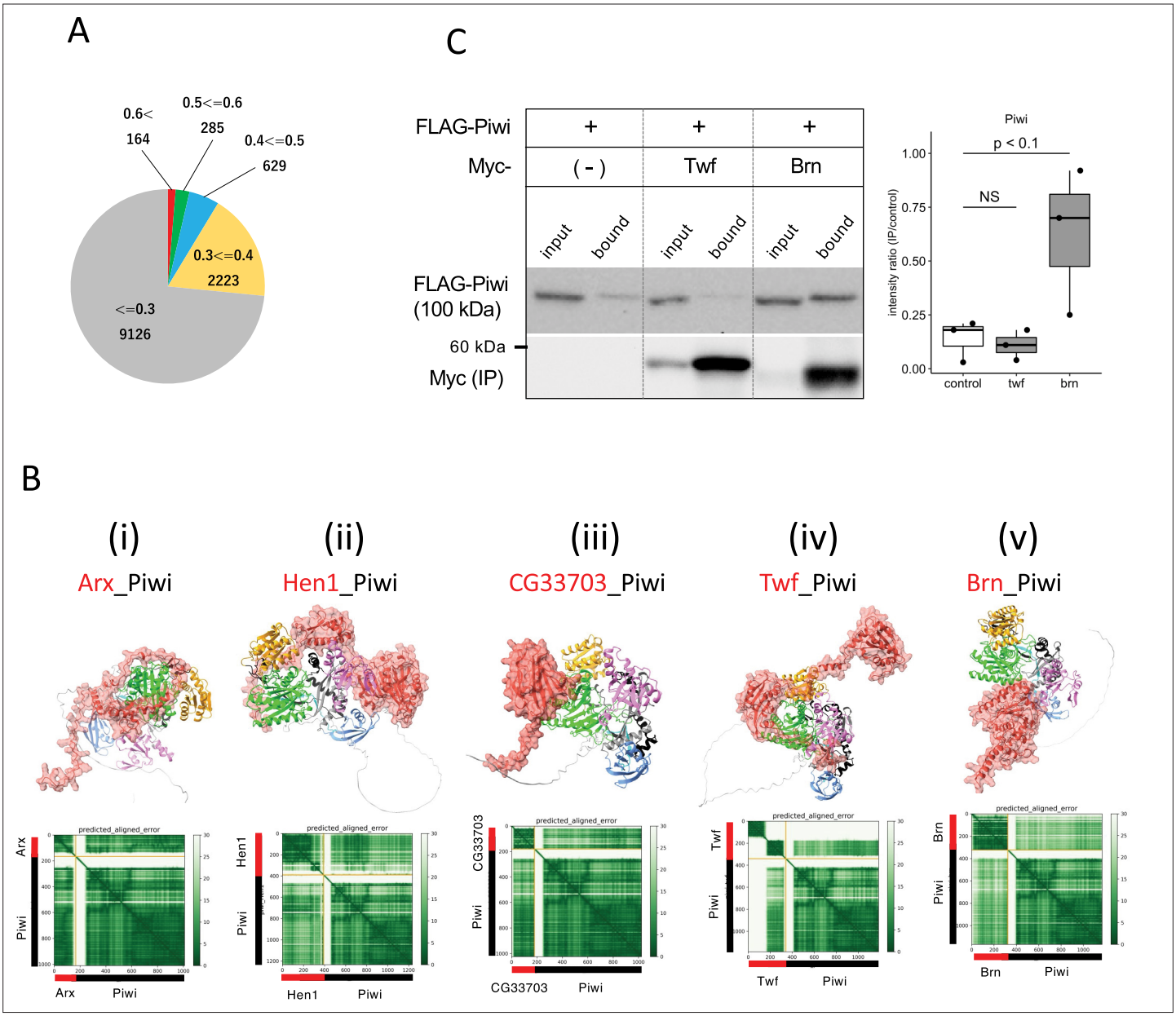

Figure 5. Screening for Piwi-interacting proteins in *Drosophila* proteome. (**A**) Pie chart displaying the distribution of ranking confidences from the AlphaFold2 screening for Piwi-interacting proteins among those encoded by *Drosophila* genome. (**Bi–v**) The predicted dimer structure (top) and PAE plots (bottom) for the Piwi and the binding candidates in red: Arx (**i**), Hen1 (**ii**), CG33703 (**iii**), Twf (**iv**), and Brn (**v**). Piwi is shown in the same colors as ***Figure 5—figure supplement 1A***. (**C**) Co-immunoprecipitation assays using tagged proteins to verify interactions between Piwi and the binding candidates, Twf and Brn. Single transfected cells expressing only Flag-Piwi is used as negative control. Box and whisker plots show the intensity ratio between immunoprecipitated and input bands (n = 3 biological replicates). p-values were calculated using Student's *t*-test.

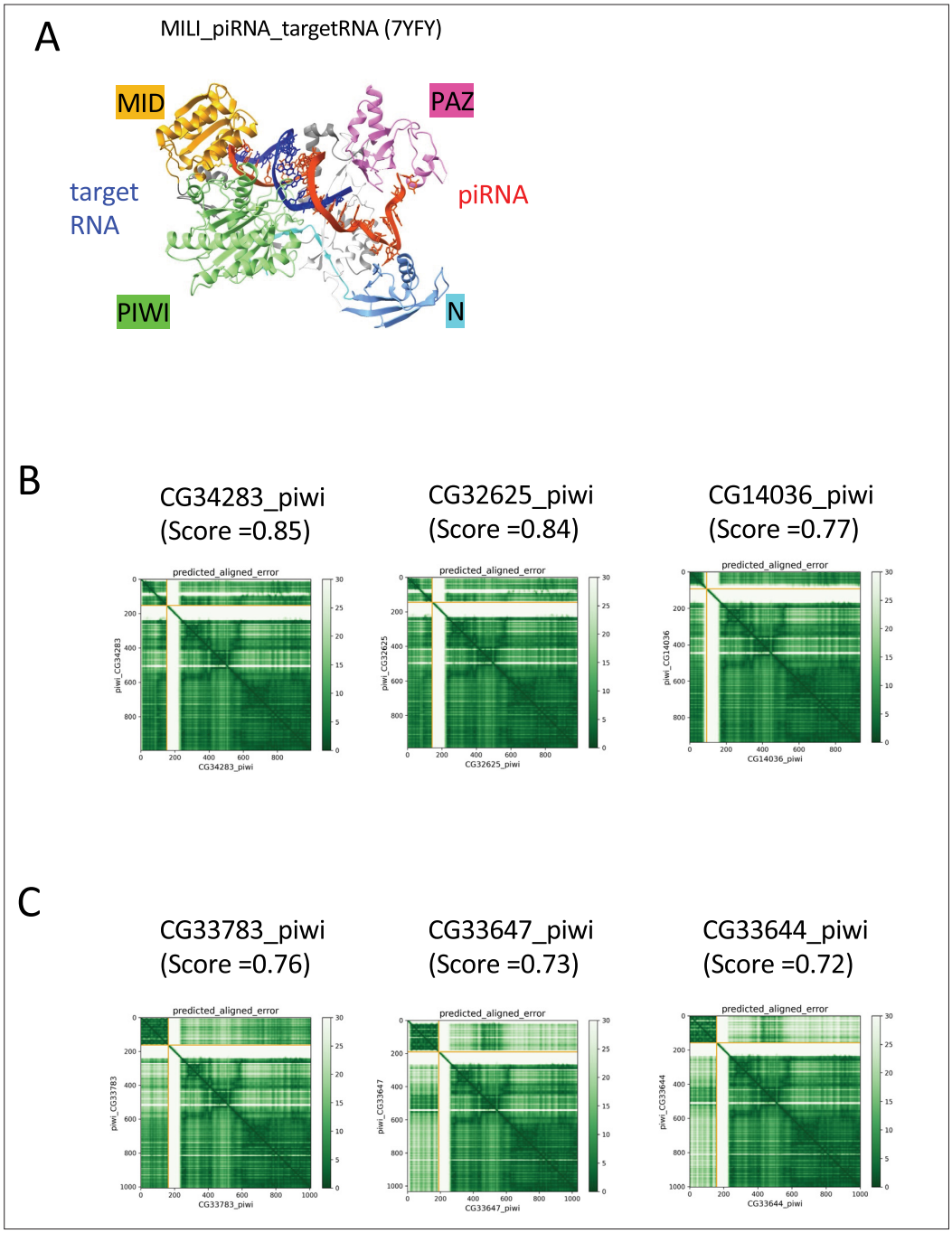

Figure 5—figure supplement 1. Structural analyses of Piwi complexes and interactions. (**A**) The ternary complex of mouse Piwi ortholog (MILI), piRNA, and the target RNA determined by cryo-EM (PDB: 7YFY). (**B**) PAE plots for the predicted dimer structures of Piwi and Arx paralogs in *Drosophila melanogaster*. (**C**) PAE plots for the predicted dimer structures of Piwi and CG33703 paralogs in *Drosophila* melanogaster.